metals

MDPI

Article

Numerical Study about the Influence of Superimposed Hydrostatic Pressure on Shear Damage Mechanism in Sheet Metals

Mohammadmehdi Shahzamanian [1,2,*], Chris Thomsen [3], Amir Partovi [1], Zhutian Xu [4] and Peidong Wu [1]

[1] Department of Mechanical Engineering, McMaster University, Hamilton, ON L8S 4L7, Canada; partovia@mcmaster.ca (A.P.); peidong@mcmaster.ca (P.W.)
[2] Department of Civil and Environmental Engineering, University of Alberta, Edmonton, AB T6G 2W2, Canada
[3] Department of Materials Engineering, NORAM Engineering and Constructors Ltd., Vancouver, BC V6C 1S4, Canada; cthomsen@noram-eng.com
[4] School of Mechanical Engineering, Shanghai Jiao Tong University, Shanghai 200240, China; zhutianxu@sjtu.edu.cn
* Correspondence: mmshahzamanian@gmail.com or mshahzam@ualberta.ca

check for updates

Citation: Shahzamanian, M.; Thomsen, C.; Partovi, A.; Xu, Z.; Wu, P. Numerical Study about the Influence of Superimposed Hydrostatic Pressure on Shear Damage Mechanism in Sheet Metals. *Metals* **2021**, *11*, 1193. https://doi.org/10.3390/met11081193

Academic Editors: Antonio Mateo, Giovanni Meneghetti and Filippo Berto

Received: 6 June 2021
Accepted: 23 July 2021
Published: 27 July 2021

Abstract: It is generally accepted that the superimposed hydrostatic pressure increases fracture strain in sheet metal and mode of fracture changes with applying pressure. Void growth is delayed or completely eliminated under pressure and the shear damage mechanism becomes the dominant mode of fracture. In this study, the effect of superimposed hydrostatic pressure on the ductility of sheet metal under tension is investigated using the finite element (FE) method employing the modified Gurson–Tvergaard–Needleman (GTN) model. The shear damage mechanism is considered as an increment in the total void volume fraction and the model is implemented using the VUMAT subroutine in the ABAQUS/Explicit. It is shown that ductility and fracture strain increase significantly by imposing hydrostatic pressure as it suppresses the damage mechanisms of microvoid growth and shear damage. When hydrostatic pressure is applied, it is observed that although the shear damage mechanism is delayed, the shear damage mechanism is dominant over the growth of microvoids. These numerical findings are consistent with those experimental results published in the previous studies about the effect of superimposed hydrostatic pressure on fracture strain. The numerical results clearly show that the dominant mode of failure changes from microvoid growth to shear damage under pressure. Numerical studies in the literature explain the effect of pressure on fracture strain using the conventional GTN model available in the ABAQUS material behavior library when the mode of fracture does not change. However, in this study, the shear modified GTN model is used to understand the effect of pressure on the shear damage mechanism as one of the individual void volume fraction increments and change in mode of fracture is explained numerically.

Keywords: superimposed hydrostatic pressure; shear damage growth; fracture strain; finite element analysis (FEA)

1. Introduction

There are several methods of increasing the ductility of metals, such as superimposing hydrostatic pressure [1,2]. In mechanical testing under superimposed hydrostatic pressure, tensile testing of the specimen is carried out in a pressure vessel that applies the desired level of pressure in the load assembly [3]. The effect of superimposed hydrostatic pressure has been studied numerically using the conventional Gurson–Tvergaard–Needleman (GTN) model under tension and bending in previous studies [1–4]. However, in this study, the modified GTN model considering the shear damage growth as an increment in the void volume fraction is used to investigate the effect of superimposed hydrostatic pressure on the shear damage mechanism.

The different failure modes shown in Figure 1 can be described in terms of the ratio of shear and normal stresses. Generally, shear failure is dominant for low or zero stress triaxiality, while the process of void nucleation, growth, and coalescence occurs when stress triaxiality is high [5]. Ashby et al. [6] investigated the influence of pressure and temperature on damage in terms of the of brittle, fully plastic, ductile, and shear fracture mechanisms. It was shown that the failure mode is a function of pressure and temperature, with an increase in pressure corresponding to an increase in ductility. It was also demonstrated that a material only fails in a fully plastic manner when all other fracture mechanisms are suppressed. This failure mode is characterized by the onset of necking that progresses to a point of zero area when a material is continuously loaded in tension past its yield point. Kao et. Al [7] used quantitative metallography to determine the effect of hydrostatic pressure on the failure mode of a steel subjected to tensile deformation. It was observed that a superimposed hydrostatic pressure suppressed the nucleation of voids and resulted in a significant increase in ductility. Unlike the void-sheet mechanism, shear decohesion is not strongly influenced by pressure; this causes the latter to be the only valid mechanism to explain the observed failure [7]. Overall, it is generally accepted that a superimposed hydrostatic pressure increases ductility by delaying or completely eliminating void nucleation and growth; this matter has been investigated in other studies [6,8–12].

Figure 1. Different types of fracture mechanisms controlled by shear stress and normal stress and their combinations [5].

For many high-strength sheet materials, such as aluminum alloys that contain a significant amount of second phase particles, microvoids often develop in the vicinity of these particles during large plastic deformation. These particle-induced microvoids are known to localize plastic flow and limit the formability of sheet metals [13–16]. One of the well-known models of ductile void growth that is often utilized in analyzing large plastic deformation of ductile metallic materials is the Gurson–Tvergaard–Needleman (GTN) model, proposed by Tvergaard and Needleman [17] as an improvement on the accuracy of the original Gurson model [18]. These models treat voids as spherical cavities and capture their effects on material yield following a modification of the von Mises yield criterion [18]. More recently, the GTN model has been extended to include the effect of shear damage by Nahshon and Hutchinson [19]. Sun et al. [20] used the shear modified GTN model and simulated punch test and identified the parameters using the neural networking. The size effect on damage evolution using the shear modified GTN model under high/low stress triaxiality is performed by Li et al. [21]. Yildiz and Yilmaz [22] used the shear modified GTN model to simulate the plastic deformation for 6061 aluminum alloys. Overall, the shear modified GTN model has been used frequently to simulate various materials for different tests [23–27].

Peng et al. [4] investigated the effect of superimposed hydrostatic pressure on fracture in round bars. It was shown that, because void formation is not significant prior to necking, superimposed pressure has little or no effect on the yield strength of metals.

However, the numerical results showed that due to a suppression in void nucleation and growth by the applied pressure, the fracture strain increased, and the failure process was extended. The effect of superimposed pressure on fracture in sheet metals under tension was studied in [3], where it was again found that the application of hydrostatic pressure increased the ductility in sheet metal. Numerical results showed the transition of fracture surface from planar mode at atmospheric pressure to chisel mode under high pressure as observed experimentally.

The effect of superimposed hydrostatic pressure on the bendability of sheet metals using the GTN model in ABAQUS is investigated in [1]. This study explored how hydrostatic pressure suppresses void growth and leads to an increase in ductility in sheet metals. The pressure and stress triaxiality were shown to decrease with an increase in superimposed hydrostatic pressure. As already mentioned, the void growth decreases, and it causes the fracture strain to increase. In another study [28], the effect of cladding on the ductility of sheet metals was investigated using the GTN model. A softer material with a higher ductility than the substrate metal was applied with perfect bonding. It was demonstrated that the application of the soft ductile layer improved the bendability of the base metal. From these two studies [1,28], it is clear that combining finite element methods (FEM) with the GTN model is a useful and successful approach to perform a range of analyses and to understand various effects on the ductility of metals in three-point bending tests.

The shear damage mechanism is a dominant mode of fracture under pressure as void growth is delayed or completely eliminated. To the best of the authors' knowledge, the effect of superimposed hydrostatic pressure on the shear damage mechanism has not been reported elsewhere. The aim of this paper was to perform a numerical study of the effect of a superimposed hydrostatic pressure on shear fracture in sheet metal under tension. The effect of superimposed pressure is explained in detail and in a step-wise manner, and it is shown what happens when the shear damage mechanism becomes a dominant mode of fracture with increasing pressure. All the simulations presented in this study were performed using ABAQUS/Explicit [29] based on the modified GTN model implemented in a VUMAT subroutine. The effect of hydrostatic pressure on the change in failure mode is explained in detail. The numerical results were found to be in good agreement with experimental observations considering the mixed dimple/shear mode of fractures in a sheet metal. The void growth and shear void growth volume fractions are considered individually in the shear modified GTN model. Therefore, the effect of pressure on void growth and shear void growth volume fractions are studied and compared with each other.

2. Constitutive Model

The Gurson–Tvergaard–Needleman (GTN) model [17,30,31] is used in this study, which is on the basis of damage growth in metals due to void nucleation, growth, and coalescence. The void growth is a function of the plastic strain rate $\mathbf{D}^P$:

$$\left(\dot{f}\right)_{growth} = (1-f)\mathbf{I} : \mathbf{D}^P \tag{1}$$

and the void nucleation is assumed to be strain controlled as follows:

$$\left(\dot{f}\right)_{nucleation} = \overline{A}\dot{\overline{\varepsilon}}^P \tag{2}$$

where $\dot{\overline{\varepsilon}}^P$ is the effective plastic strain rate, and the parameter $\overline{A}$ is chosen so that nucleation follows a normal distribution as suggested by Chu and Needleman [32]:

$$\overline{A} = \frac{f_N}{S_N\sqrt{2\pi}} exp\left[-\frac{1}{2}\left(\frac{\overline{\varepsilon}^p - \varepsilon_N}{S_N}\right)^2\right] \tag{3}$$

here, f_N is the volume fraction of void nucleating particles, ε_N is the average void nucleating strain, and S_N is the standard deviation of the void nucleating strain.

Additionally, the shear damage growth proposed by Nahshon and Hutchinson [19] is as follows:

$$df_{Shear\ damage} = k_w w(\sigma_{ij}) f \frac{S_{ij} d\varepsilon_{ij}^{p}}{\sigma_{ef}} \tag{4}$$

k_w is the magnitude of the damage growth rate in the pure shear test. The function $w(\sigma_{ij})$ identifies the current state of stress, which is defined as $w(\sigma_{ij}) = 1.0 - \left(\frac{27J_3}{2\sigma_{eq}^3}\right)^2$, where J_3 is the third invariant of the deviatoric stress matrix.

The growth of existing voids and the nucleation of new voids are considered in the evolution of void volume fraction as follows:

$$\dot{f} = \left(\dot{f}\right)_{growth} + \left(\dot{f}\right)_{nucleation} + \left(\dot{f}\right)_{shear\ damage} \tag{5}$$

and the function of void volume fraction $(f^*(f))$ is defined to consider coalescence as follows:

$$f^* = \begin{cases} f & for\ f \leq f_c \\ f_c + \frac{f_u^* - f_c}{f_f - f_c}(f - f_c) & for\ f > f_c \end{cases} \tag{6}$$

where f_c is the critical void volume fraction for coalescence and f_f is the void volume fraction at failure. The parameter $f_u^* = \frac{1}{q_1}$ is defined. It should be mentioned that void growth and nucleation does not happen when the stress state of an element is compressive; it may only occur in tension.

Finally, the approximate yield function to be used in which f^* is distributed randomly is as follows:

$$\Phi(\boldsymbol{\sigma}, \overline{\sigma}, f) = \frac{\sigma_e^2}{\overline{\sigma}^2} + 2f^* q_1 cosh\left(\frac{3q_2\sigma_H}{2\overline{\sigma}}\right) - \left[1.0 + (q_2 f^*)^2\right] = 0 \tag{7}$$

where $\boldsymbol{\sigma}$ is the macroscopic Cauchy stress tensor and σ_e, σ_H, and $\overline{\sigma}$ are the equivalent stress, hydrostatic stress, and matrix stress, respectively. In fact, the matrix stress and equivalent stresses are damaged and undamaged stresses in the GTN model. Additionally, q_1 and q_2 are calibrated parameters.

The uniaxial elastic–plastic undamaged stress–strain curve for the matrix material is provided by the following power-law form:

$$\overline{\varepsilon} = \begin{cases} \frac{\overline{\sigma}}{E}, & for\ \overline{\sigma} \leq \sigma_y \\ \frac{\sigma_y}{E}\left(\frac{\overline{\sigma}}{\sigma_y}\right)^n, & for\ \overline{\sigma} > \sigma_y \end{cases} \tag{8}$$

3. Problem Formulation and Method of Solution

A sheet metal with length L_o, thickness t_o, and width W_o that is under hydrostatic pressure is considered and shown schematically in Figure 2. It is assumed that the sheet is wide enough and that no deformation occurs in the width direction, such that the sheet may be considered to be under plane strain. The shear modified GTN model is not supported in the ABAQUS material behavior library and a VUMAT subroutine was implemented in this study to investigate the effect of pressure on shear damage mechanism. However, the subroutine only supports the three-dimensional elements. The superimposed hydrostatic pressure is represented by small brown arrows directed into the material from all directions. The sequence of tensile strain under superimposed hydrostatic pressure is modeled as two steps. In the first step, the pressure is gradually increased up to a desired level $p = -\alpha\sigma_y$ (α defines the value of applied pressure respect with yield stress) without applying any tensile strain. In the second step, tensile strain is applied to the sheet while maintaining the constant pressure value $p = -\alpha\sigma_y$.

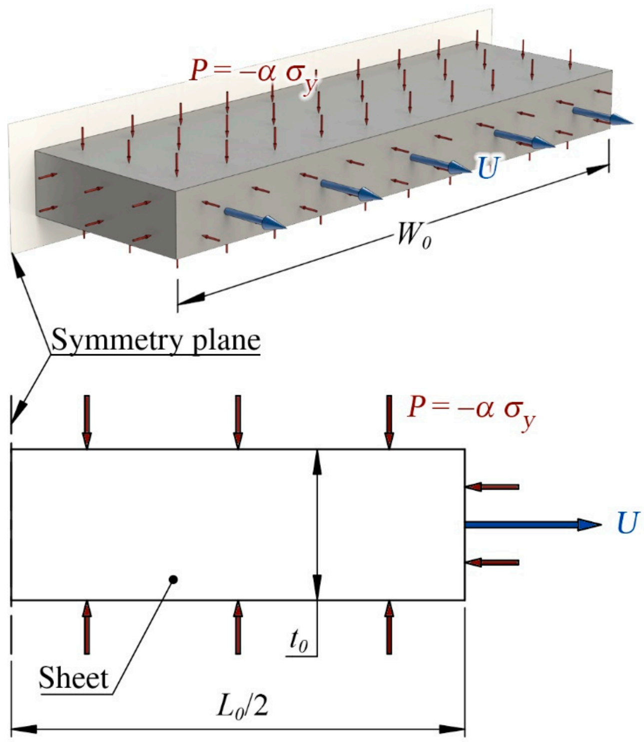

Figure 2. Schematic of a sheet metal under superimposed hydrostatic pressure.

The elastic–plastic properties of the matrix material are specified by $\sigma_y/E = 0.0033$, $\nu = 0.3$ and $n = 10$. It is assumed that the initial void volume fraction is zero and the fit parameters in the GTN model (Equation (7)) are $q_1 = 1.5$ and $q_2 = 1.0$. These values for q_1 and q_2 were found to be in good agreement in [31] for metals to analyze the bifurcation mode of porous metals. Void nucleation is assumed to be plastic strain controlled, the volume fraction of void nucleating particles $f_N = 0.04$, the mean strain for void nucleation $\varepsilon_N = 0.3$, and the corresponding standard deviation $S_N = 0.1$. The parameters related to the final failure, f_c and f_f, are assumed to be 0.15 and 0.25, respectively. These values of mechanical properties are taken from Tvergaard and Needleman [17]. It should be emphasized that the main purpose of the present study is to assess the effect of superimposed hydrostatic pressure on the ductility of sheet metals and particularly on the shear damage mechanism, and that the overall results and conclusions are not particularly dependent on the above values of the material parameters. The three-dimensional element C3D8R in ABAQUS/Explicit is used for the sheet. The mass scaling method with a sufficient low target time increment is used and it is carefully attempted to minimize the dynamic effect of the sample. Therefore, a wide sheet with a width (W_o) of 100 mm is considered when the length (L_o) and thickness (t_o) are 60 mm and 10 mm, respectively. It is to be noted that all nodes in the sheet are constrained in the width direction.

As the mesh sensitivity is expected in numerical simulations involving localized deformation and fracture, different meshes are considered in this simulation. Figure 3 shows the finite element (FE) configuration of the specimen with a typical mesh for metal sheet consisting of $60 \times 110 \times 4$ elements (60 elements in thickness direction, 110 elements in length direction and 4 elements in width direction) in which the element distribution in the refined area is biased to the middle section of the specimen where fracture is expected to occur. Due to the symmetry, only half of the sheet is investigated and symmetric boundary conditions are imposed in the middle section of specimen. Figure 4 represents the normalized force (F^*) as a function of the tensile strain ε for fully base material and the effect of mesh sensitivity on this curve is also included. Force is normalized by the multiplication of the yield stress of the material and the initial cross section of the sheet, and $\varepsilon = \ln\left(1.0 + \frac{\Delta l}{l_o}\right)$.

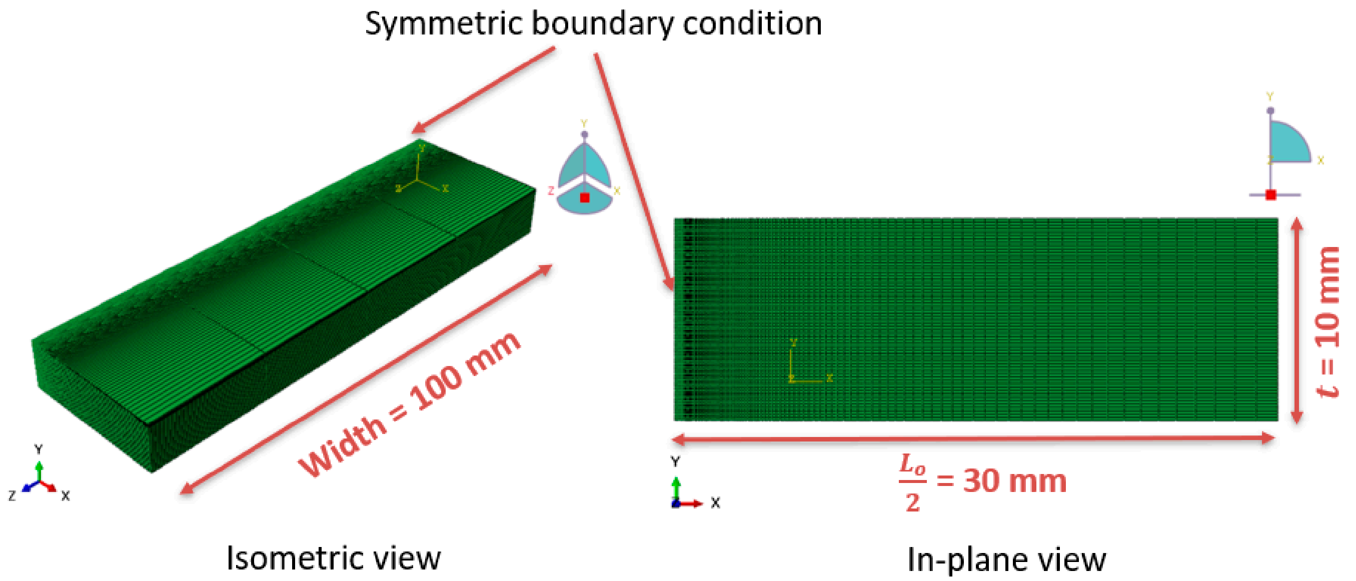

Figure 3. Finite element (FE) configuration of a specimen under tension.

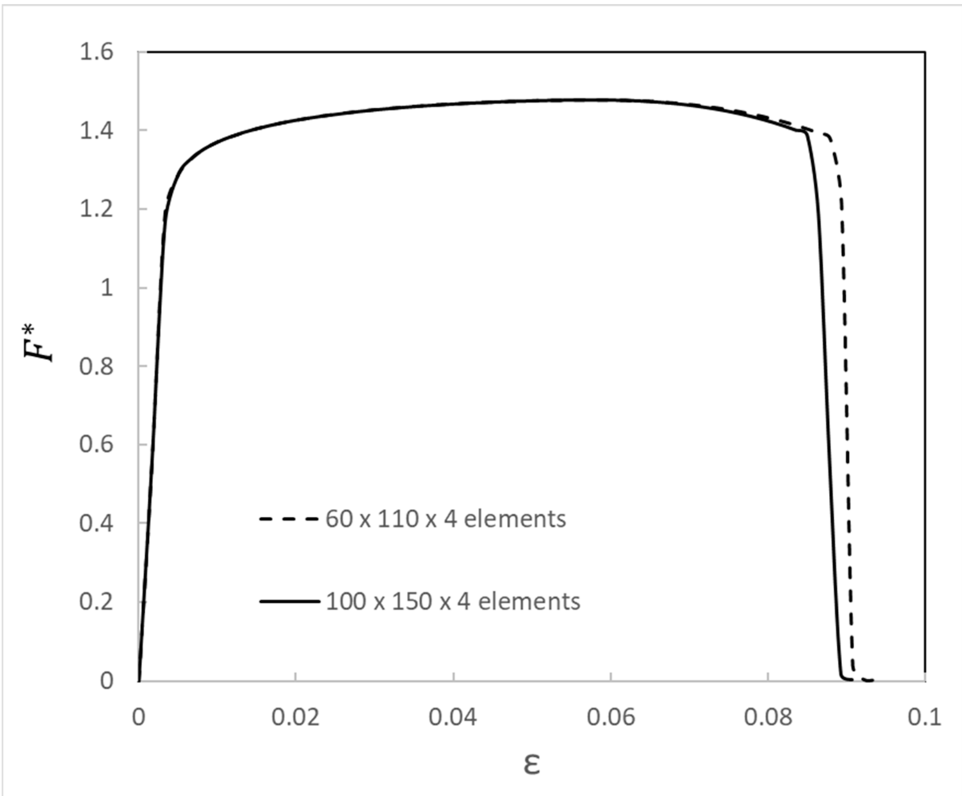

Figure 4. Effect of mesh sensitivity on force–tensile strain.

4. Results and Discussion

In this section, the 60 × 110 × 4 elements mesh distribution is used to present the results. The effect of k_w on the force as a function of tensile strain under ambient pressure ($\alpha = 0.0$) is shown in Figure 5. It is clearly observed that the fracture delays with a decrease in k_w. Shear damage growth increases with an increase in k_w according to Equation (4). Therefore, the total void volume fraction increases with k_w as shown in Equation (5). It should be noted that the result for the case with $k_w = 0.0$ corresponds to using the conventional GTN model with the effect of shear damage mechanism not being considered. Additionally, the deformed shape of the fractured specimen is shown in Figure 6. Necking and localized deformation is clearly observed in the specimen. Damage is very low, close to zero, before necking and it starts to grow when localized deformation happens.

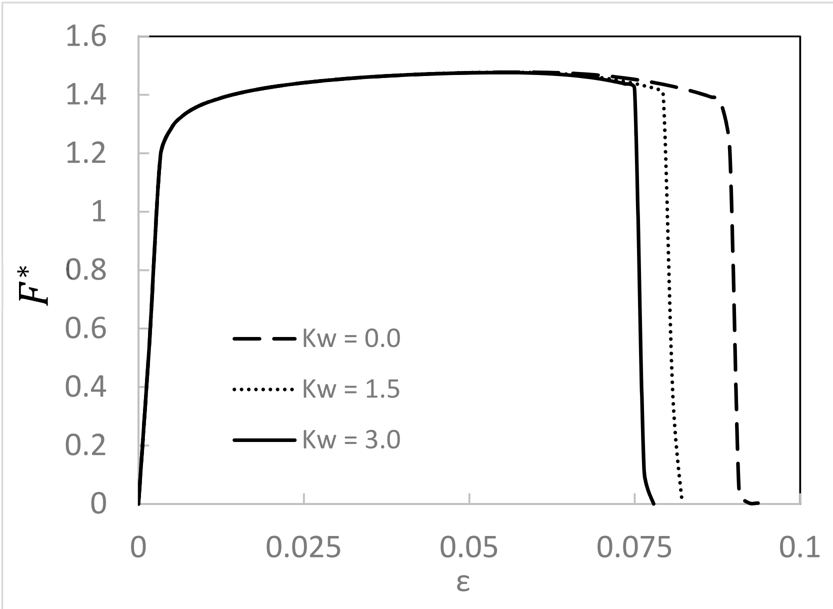

Figure 5. Effect of k_w on the normalized force–tensile strain curve.

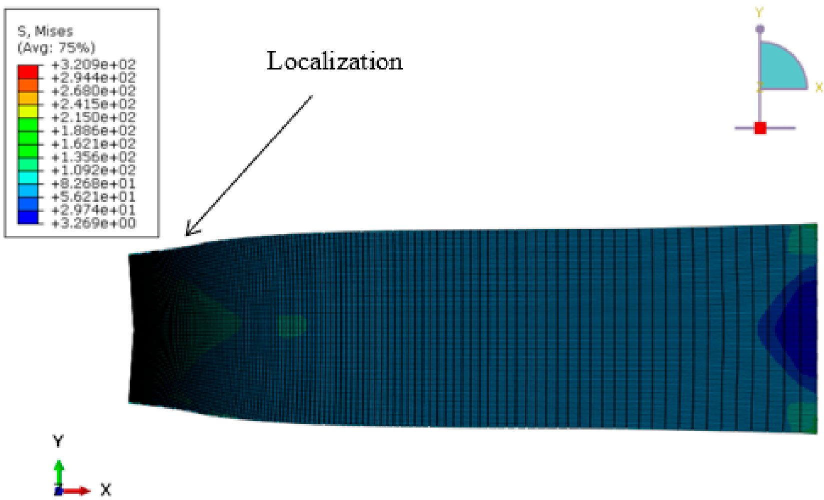

Figure 6. Deformed shape of the specimen after fracture.

As mentioned previously, the effect of pressure on ductility and bendability has been determined in [1,4] using the conventional GTN model when the effect of the shear damage mechanism is not considered. It is explained in [1,4] that the superimposed hydrostatic pressure lowers the stress triaxiality, which retards void growth and increases the fracture strain. In the present study, the influence of superimposed hydrostatic pressure $(p = -\alpha\sigma_y)$ on fracture under tension is considered while accounting for the shear damage mechanism by using the modified GTN model. Figure 7 shows the effect of α on the force–tensile strain curve. It was found that as α increases, the tensile strength is unaffected and the fracture strain of the material increases.

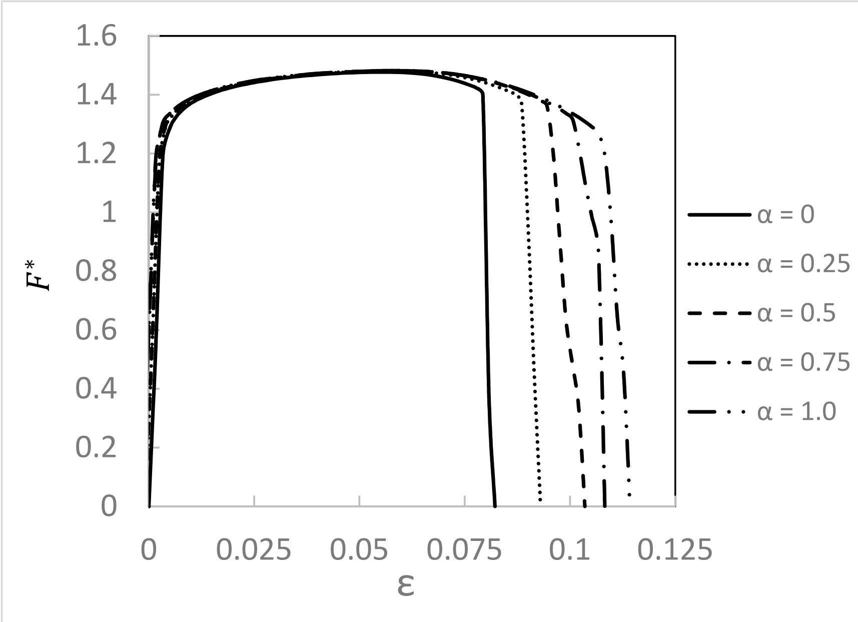

Figure 7. Effect of superimposed hydrostatic pressure on normalized force–tensile strain curves.

Figure 8 shows the volumetric strain $(\varepsilon_{11} + \varepsilon_{22} + \varepsilon_{33})$ at the center of the specimen for sheets under a range of superimposed hydrostatic pressures. It is found that the volumetric strain decreases with increasing α as shown in Figure 8. According to Equation (1), the decrease in volumetric strain renders void growth less favorable and leads to higher ductility.

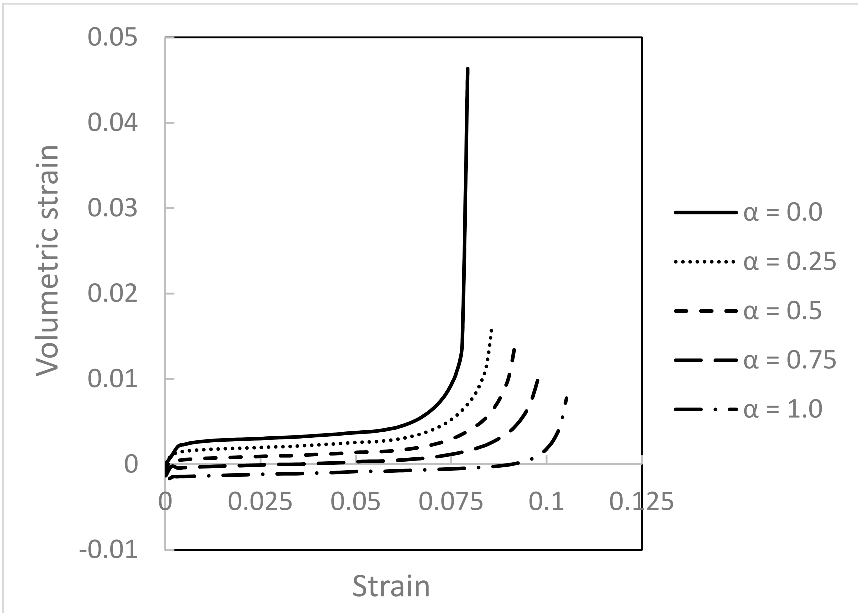

Figure 8. Effect of superimposed hydrostatic pressure on volumetric strain at the center of the specimen.

The delay of void growth and the concomitant increase in fracture strain caused by the increase in applied pressure can be explained in terms of how this pressure influences the hydrostatic pressure and stress triaxiality at the center of the specimen. Figure 9 presents the hydrostatic pressure $\sigma_H = (1/3)(\sigma_{xx} + \sigma_{yy} + \sigma_{zz})$ and stress triaxiality $\frac{\sigma_H}{\bar{\sigma}}$ at the center of the specimen, where fracture initiates as a function of tensile strain under various superimposed hydrostatic pressures. At room pressure $p = 0$, both hydrostatic pressure and stress triaxiality develop in a way to assist void growth. However, under a superimposed hydrostatic pressure $p = -\alpha\sigma_y$, both values are initially compressive. This result implies that void growth is delayed until a sufficiently large component of tensile stress is introduced.

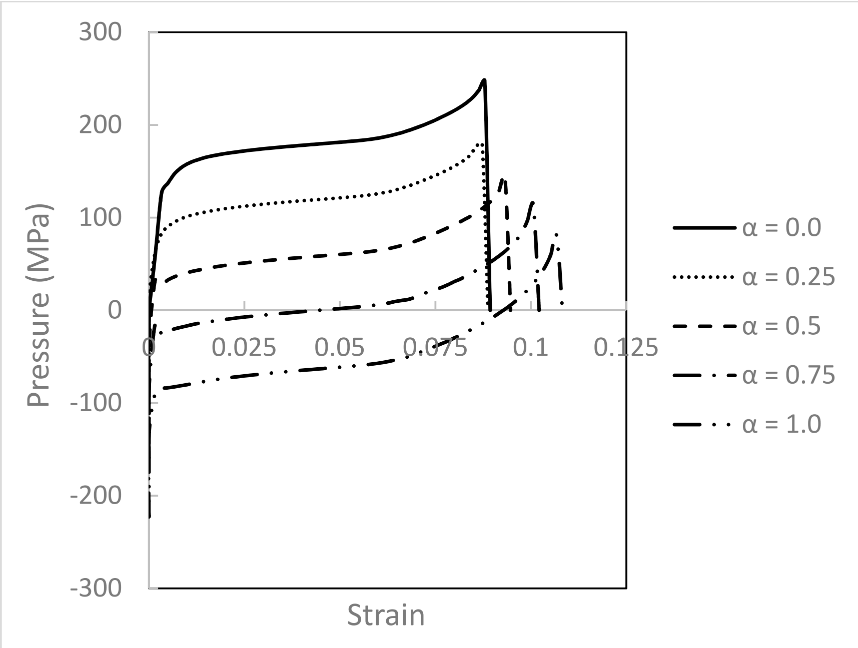

(**a**) Hydrostatic pressure

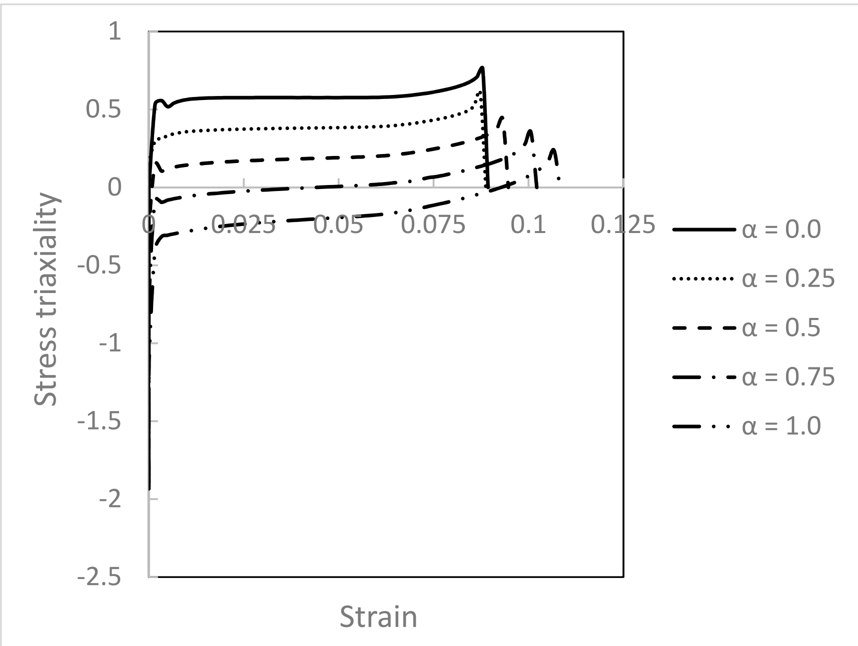

(**b**) Stress triaxiality

Figure 9. Effect of superimposed hydrostatic pressure on (**a**) pressure and (**b**) stress triaxiality at the center of the specimen.

The effect of superimposed double-sided pressure on the formability of a biaxially stretched age-hardenable aluminum sheet metal (AA6111-T4) was studied in [33], where the researchers numerically employed the GTN model. It was found that double-sided pressure increased formability while void nucleation remained invariable. Furthermore, only the extent of void growth was observed to change, decreasing with an increase in pressure. Figure 10a shows the effect of superimposed hydrostatic pressure on void nucleation. It is demonstrated that the final value of nucleated void volume fraction is not a function of superimposed hydrostatic pressure as the GTN model used in this study assumes that the nucleation is strain controlled (Equations (2) and (3)). A previous study [1] investigated the effect of superimposed hydrostatic pressure on bendability by using both the strain- and stress-controlled void nucleating GTN model. It was found that the final value of nucleating void volume fraction is constant when the strain void nucleating GTN model is used [1]. On the contrary, the final value of nucleating void volume fraction decreases with increasing pressure when the stress-controlled void nucleating GTN model is used. However, the effect of superimposed hydrostatic pressure on void growth is shown in Figure 10b and it is clearly seen that hydrostatic pressure delays void growth. The reduction in void growth due to an increase in the hydrostatic pressure has been reported in other studies for sheets under tension [4] and bending [28]. Figure 10c shows the effect of hydrostatic pressure on the prevalence of the shear damage mechanism and it is clearly observed that it dominates at higher values of hydrostatic pressure. As mentioned previously, the void sheet mechanism is excluded under external applied pressure, leaving shear decohesion as the dominant failure mechanism [7]. It is interesting to note that while the shear damage mechanism becomes more dominant as pressure is increased, both it and the void growth mechanism calculated using the modified GTN model become more delayed as the superimposed hydrostatic pressure is increased. Finally, Figure 10d shows the total void volume fraction under various superimposed hydrostatic pressures. It is found that the total void volume fraction delays and it will be shown that it causes the fracture strain to increase.

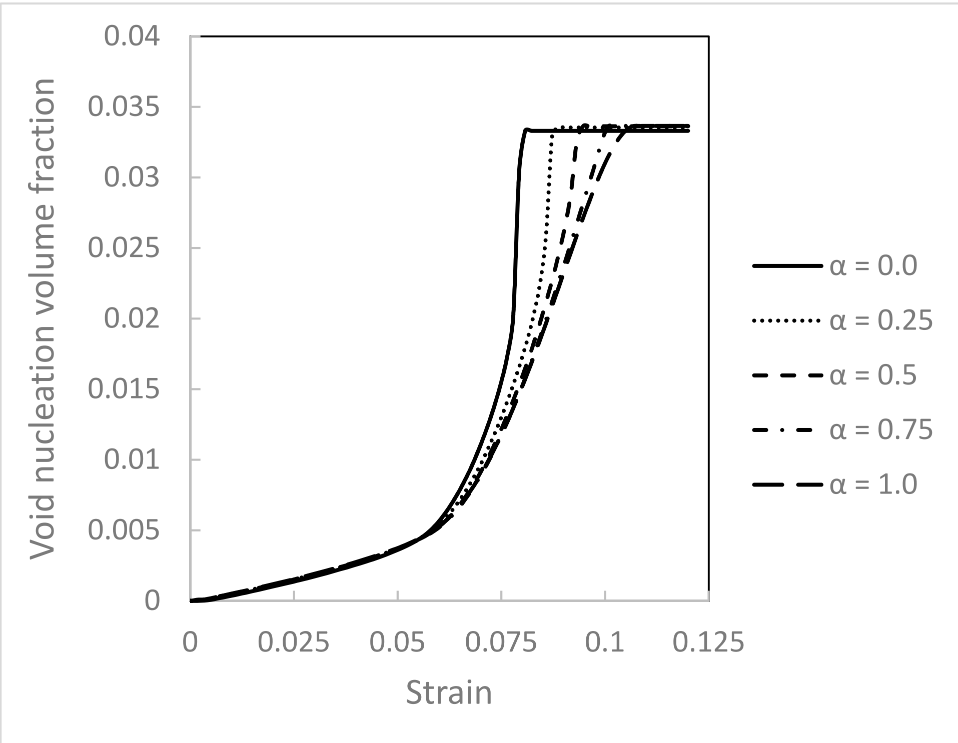

(**a**) Void nucleation volume fraction

Figure 10. *Cont*.

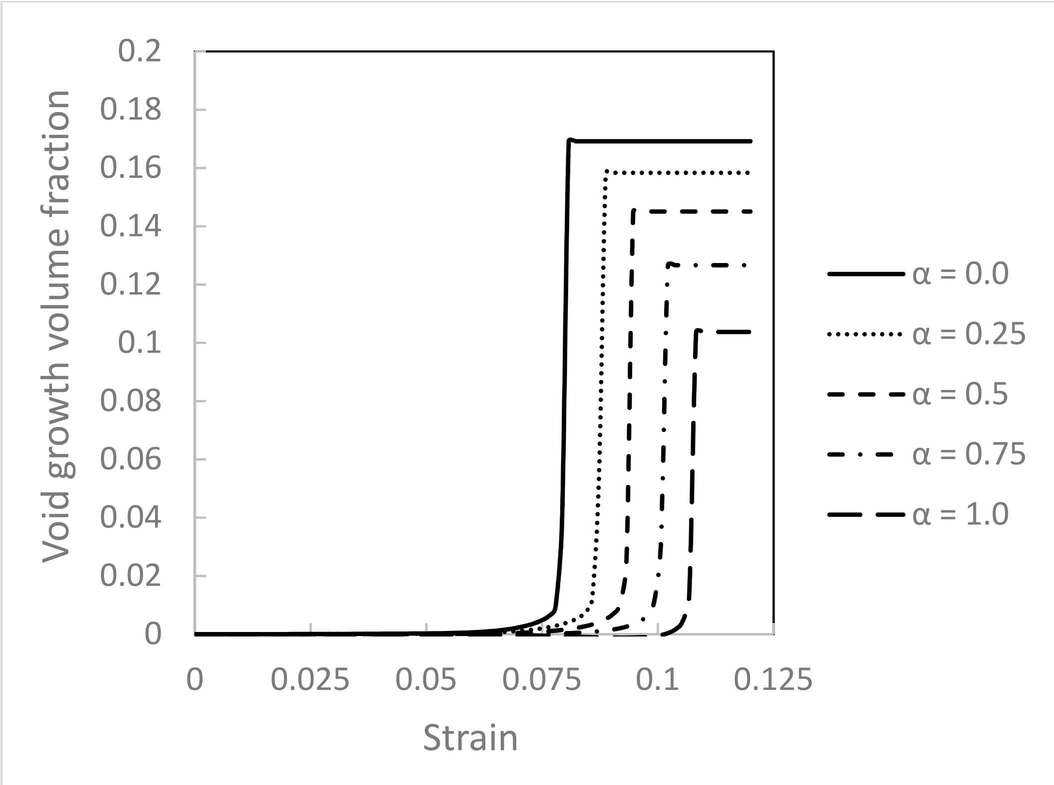

(**b**) Void growth volume fraction

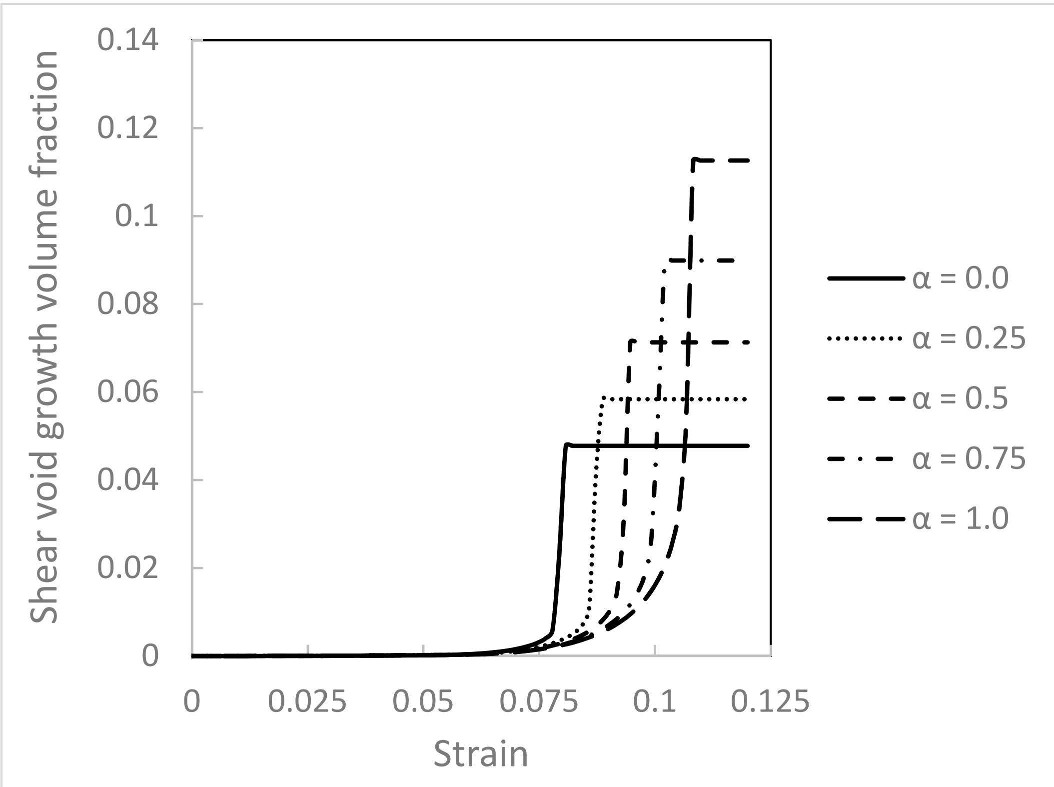

(**c**) Shear void growth volume fraction

Figure 10. *Cont*.

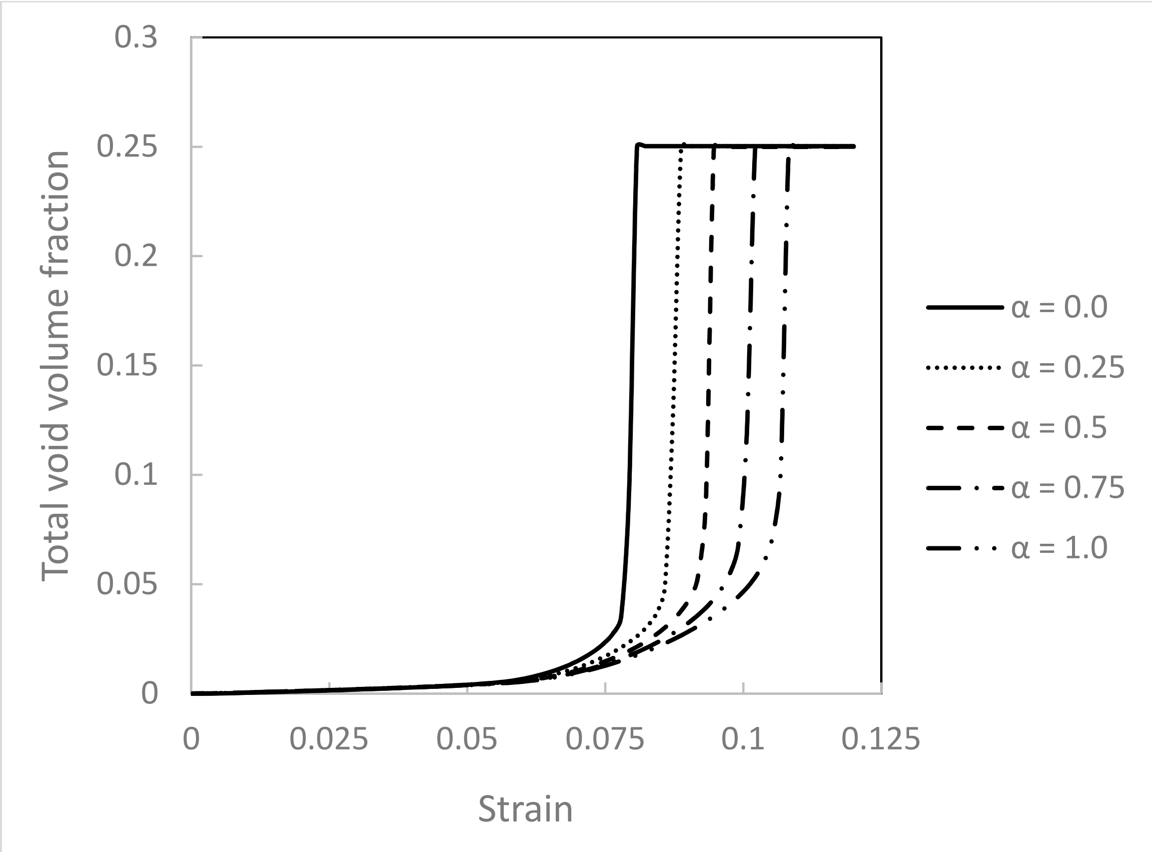

(**d**) Total void volume fraction

Figure 10. Effect of superimposed hydrostatic pressure on (**a**) void nucleation volume fraction, (**b**) void growth volume fraction, (**c**) shear void growth volume fraction and (**d**) total void volume fraction at the center of the specimen.

Figures 11 and 12 plot the influence of superimposed hydrostatic pressure on the normalized minimum cross-section area $\left(\frac{A_{min}}{A_o}\right)$ and the fracture strain $\left(\varepsilon_f\right)$ in the middle section of the specimen, respectively. Here, the fracture strain ε_f is defined as $\varepsilon_f = \ln \frac{A_o}{A_{min}}$, where A_{min} is the minimum cross-sectional area of the sheet when fracture is complete. It is to be noted that $A_{min} = t_{min}$ and $A_o = t_o$ considering the plane strain condition and in this way, $\frac{A_o}{A_{min}} = \frac{t_o}{t_{min}}$. The following equation will be obtained to calculate ε_f:

$$\varepsilon_f = \ln \frac{t_o}{t_{min}} \tag{9}$$

It is found that the minimum cross-sectional area follows an inverse relationship with the level of hydrostatic pressure. Therefore, as the pressure increases, the minimum cross-sectional area at fracture decreases and the specimen can deform more before failure, which is manifested as an increase in fracture strain.

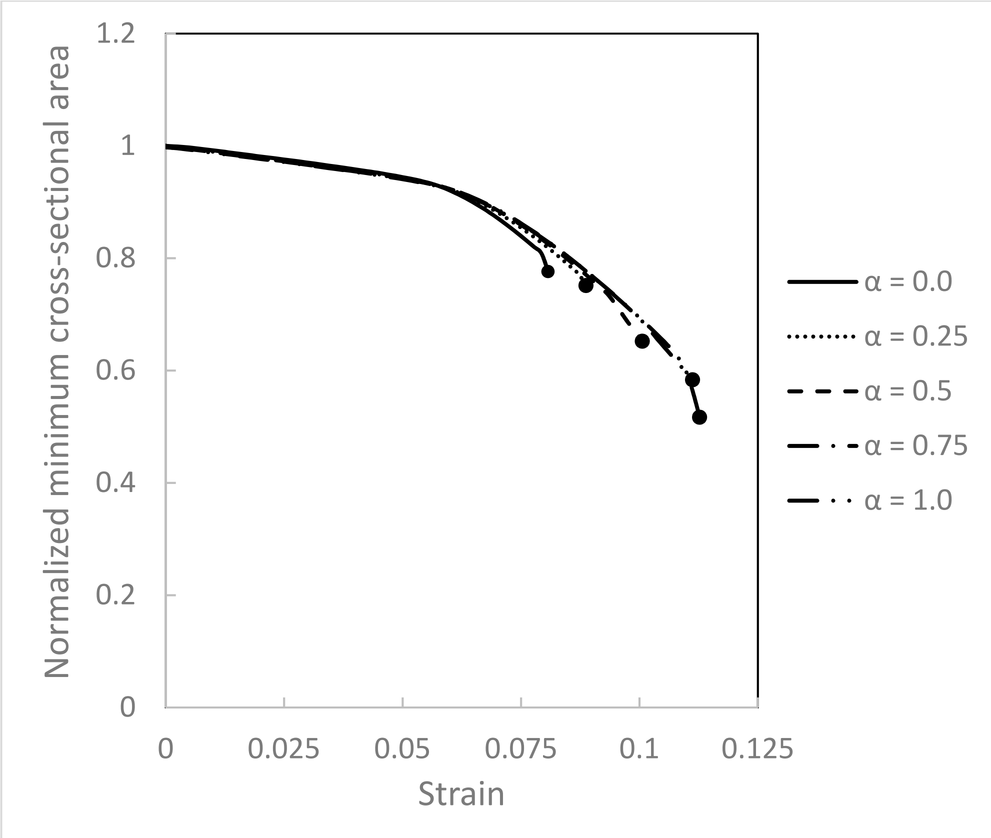

Figure 11. Effect of superimposed hydrostatic pressure on normalized minimum cross-sectional area.

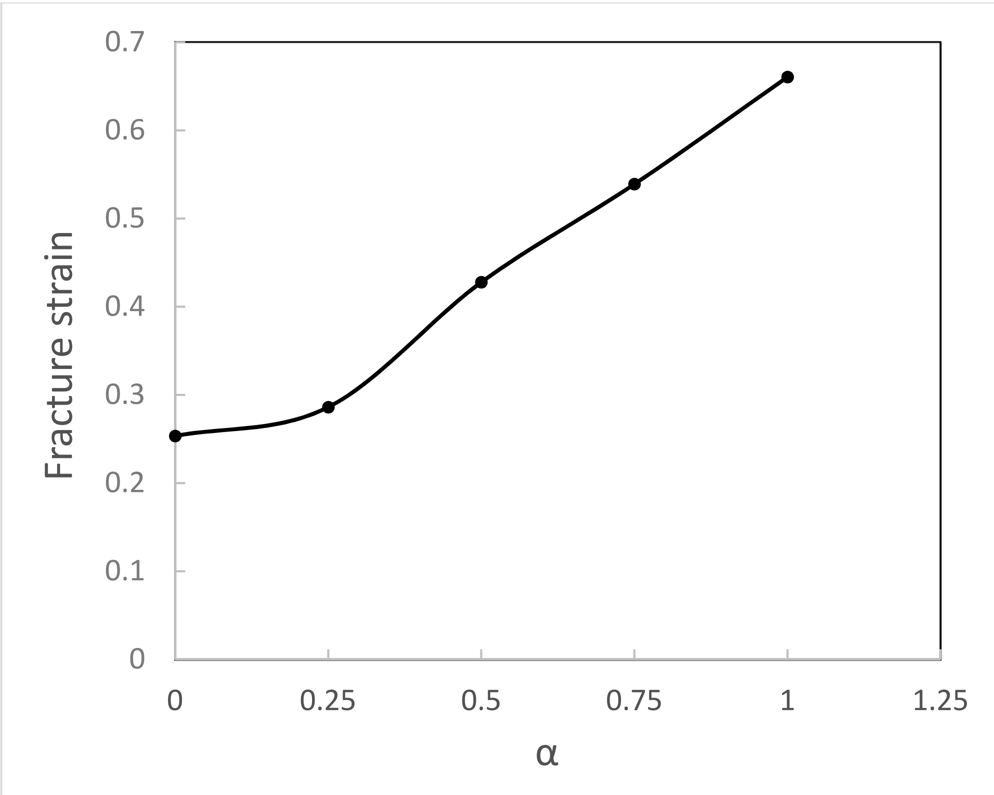

Figure 12. Effect of pressure on fracture strain.

5. Conclusions

In this study, an FEA simulation was conducted for sheet metal simultaneously subjected to a tensile test and superimposed hydrostatic pressure. The modified GTN model is used when the shear damage mechanism is considered. It is determined that the superimposed hydrostatic pressure increases the ductility significantly as hydrostatic pressure delays or eliminates growth of microvoids or microcracks as well as damage by the shear mechanism. However, it is clearly observed that the shear damage mechanism is dominant over the void growth under high pressure. The numerical results clearly show that the type of fracture changes from microvoids mechanism to shear failure under superimposed hydrostatic pressure. Finally, to sum up the conclusion remarks, the salient points are listed as follows:

- Superimposed hydrostatic pressure increases the fracture strain in metals when void growth is delayed or completely eliminated.
- Fracture mode changes under pressure and it dominates the shear damage mechanism.
- The shear modified GTN model implemented using a VUMAT subroutine explains this phenomenon when the shear damage mechanism is considered as an increment in the void volume fraction.
- Void nucleation volume fraction is constant under pressure using a strain-based void nucleating GTN model. Shear void growth volume fraction at the final fracture increases as the void growth volume fracture decreases under superimposed hydrostatic pressure.

Author Contributions: Conceptualization, M.S. and P.W.; methodology, M.S. and P.W.; software, P.W., Z.X.; validation, M.S. and P.W.; formal analysis, M.S., C.T. and P.W.; investigation, M.S., C.T. and P.W.; writing—original draft preparation, M.S., C.T., A.P., Z.X. and P.W.; writing—review and editing, M.S., C.T., A.P., Z.X. and P.W.; visualization, M.S., C.T., A.P., Z.X. and P.W.; supervision, P.W.; project administration, M.S.; funding acquisition, P.W. All authors have read and agreed to the published version of the manuscript.

Funding: This work was supported by the Natural Sciences and Engineering Research Council of Canada (NSERC, project No: RGPIN-2016-06464).

Data Availability Statement: Not applicable.

Conflicts of Interest: The authors declare no conflict of interest.

References

1. Shahzamanian, M.; Lloyd, D.; Wu, P.; Xu, Z. Study of influence of superimposed hydrostatic pressure on bendability of sheet metals. *Eur. J. Mech. A/Solids* **2021**, *85*, 104132. [CrossRef]
2. Partovi, A.; Shahzamanian, M.M.; Wu, P.D. Study of Influence of Superimposed Hydrostatic Pressure on Ductility in Ring Compression Test. *J. Mater. Eng. Perform.* **2020**, *29*, 6581–6590. [CrossRef]
3. Wu, P.D.; Chen, X.X.; Lloyd, D.J.; Embury, J.D. Effects of superimposed hydrostatic pressure on fracture in sheet metals under tension. *Int. J. Mech. Sci.* **2010**, *52*, 236–244. [CrossRef]
4. Peng, J.; Wu, P.D.; Huang, Y.; Chen, X.X.; Lloyd, D.J.; Embury, J.D.; Neale, K.W. Effects of superimposed hydrostatic pressure on fracture in round bars under tension. *Int. J. Solids Struct.* **2009**, *46*, 3741–3749. [CrossRef]
5. Kofiani, K.; Nonn, A.; Wierzbicki, T. New calibration method for high and low triaxiality and validation on SENT specimens of API X70. *Int. J. Press. Vessel. Pip.* **2013**, *111*, 187–201. [CrossRef]
6. Ashby, M.; Embury, J.; Cooksley, S.; Teirlinck, D. Fracture maps with pressure as a variable. *Scr. Met.* **1985**, *19*, 385–390. [CrossRef]
7. Kao, A.S.; Kuhn, H.A.; Richmond, O.; Spitzig, W.A. Tensile fracture and fractographic analysis of 1045 spheroidized steel under hydrostatic pressure. *J. Mater. Res.* **1990**, *5*, 83–91. [CrossRef]
8. Kao, A.; Kuhn, H.; Richmond, O.; Spitzig, W. Workability of 1045 spheroidized steel under superimposed hydrostatic pressure. *Met. Mater. Trans. A* **1989**, *20*, 1735–1741. [CrossRef]
9. French, I.E.; Weinrich, P.F. The influence of hydrostatic pressure on the tensile deformation and fracture of copper. *Met. Mater. Trans. A* **1975**, *6*, 785–790. [CrossRef]
10. French, I.; Weinrich, P.; Weaver, C. Tensile fracture of free machining brass as a function of hydrostatic pressure. *Acta Met.* **1973**, *21*, 1045–1049. [CrossRef]
11. Brownrigg, A.; Spitzig, W.; Richmond, O.; Teirlinck, D.; Embury, J. The influence of hydrostatic pressure on the flow stress and ductility of a spherodized 1045 steel. *Acta Met.* **1983**, *31*, 1141–1150. [CrossRef]

12. Korbel, A.; Raghunathan, V.; Teirlinck, D.; Spitzig, W.; Richmond, O.; Embury, J. A structural study of the influence of pressure on shear band formation. *Acta Met.* **1984**, *32*, 511–519. [CrossRef]
13. Gologanu, M.; Leblond, J.-B.; Devaux, J. Approximate models for ductile metals containing non-spherical voids—Case of axisymmetric prolate ellipsoidal cavities. *J. Mech. Phys. Solids* **1993**, *41*, 1723–1754. [CrossRef]
14. Lievers, W.B.; Pilkey, A.; Lloyd, D. The influence of iron content on the bendability of AA6111 sheet. *Mater. Sci. Eng. A* **2003**, *361*, 312–320. [CrossRef]
15. Lievers, W.B.; Pilkey, A.; Lloyd, D. Using incremental forming to calibrate a void nucleation model for automotive aluminum sheet alloys. *Acta Mater.* **2004**, *52*, 3001–3007. [CrossRef]
16. Chen, Z.T.; Worswick, M.J.; Cinotti, N.; Pikey, A.K.; Lloyd, D. A linked FEM-damage percolation model of aluminum alloy sheet forming. *Int. J. Plast.* **2003**, *19*, 2099–2120. [CrossRef]
17. Tvergaard, V.; Needleman, A. Analysis of the cup-cone fracture in a round tensile bar. *Acta Met.* **1984**, *32*, 157–169. [CrossRef]
18. Gurson, A.L. Continuum Theory of Ductile Rupture by Void Nucleation and Growth: Part I—Yield Criteria and Flow Rules for Porous Ductile Media. *J. Eng. Mater. Technol.* **1977**, *99*, 2–15. [CrossRef]
19. Nahshon, K.; Hutchinson, J. Modification of the Gurson Model for shear failure. *Eur. J. Mech. A/Solids* **2008**, *27*, 1–17. [CrossRef]
20. Sun, Q.; Lu, Y.; Chen, J. Identification of material parameters of a shear modified GTN damage model by small punch test. *Int. J. Fract.* **2020**, *222*, 25–35. [CrossRef]
21. Li, X.; Chen, Z.; Dong, C. Size effect on the damage evolution of a modified GTN model under high/low stress triaxiality in meso-scaled plastic deformation. *Mater. Today Commun.* **2021**, *26*, 101782. [CrossRef]
22. Yildiz, R.; Yilmaz, S. Experimental Investigation of GTN model parameters of 6061 Al alloy. *Eur. J. Mech. A/Solids* **2020**, *83*, 104040. [CrossRef]
23. More, S.; Kumar, A.; Narasimhan, K. Parameter identification of GTN damage model using response surface methodology for single point incremental sheet forming of IF steel. *Adv. Mater. Process. Technol.* **2021**, 1–16. [CrossRef]
24. Li, L.; Khandelwal, K. Topology Optimization of Energy-Dissipating Plastic Structures with Shear Modified Gurson–Tvergaard–Needleman Model. *J. Struct. Eng.* **2020**, *146*, 04020229. [CrossRef]
25. Singh, A.K.; Kumar, A.; Narasimhan, K.; Singh, R. Understanding the deformation and fracture mechanisms in backward flow-forming process of Ti-6Al-4V alloy via a shear modified continuous damage model. *J. Mater. Process. Technol.* **2021**, *292*, 117060. [CrossRef]
26. He, Z.; Zhu, H.; Hu, Y. An improved shear modified GTN model for ductile fracture of aluminium alloys under different stress states and its parameters identification. *Int. J. Mech. Sci.* **2021**, *192*, 106081. [CrossRef]
27. Ying, L.; Wang, D.; Liu, W.; Wu, Y.; Hu, P. On the numerical implementation of a shear modified damage model and its ap-plication to small punch test. *Int. J. Mater. Form.* **2018**, *11*, 527–539. [CrossRef]
28. Shahzamanian, M.; Lloyd, D.; Wu, P. Enhanced bendability in sheet metal produced by cladding a ductile layer. *Mater. Today Commun.* **2020**, *23*, 100952. [CrossRef]
29. *Abaqus/CAE User's Manual*; ABAQUS Inc.: Waltham, MA, USA, 2014.
30. Tvergaard, V. Influence of voids on shear band instabilities under plane strain conditions. *Int. J. Fract.* **1981**, *17*, 389–407. [CrossRef]
31. Tvergaard, V. On localization in ductile materials containing spherical voids. *Int. J. Fract.* **1982**, *18*, 237–252.
32. Chu, C.C.; Needleman, A. Void Nucleation Effects in Biaxially Stretched Sheets. *J. Eng. Mater. Technol.* **1980**, *102*, 249–256. [CrossRef]
33. Liu, J.; Wang, Z.; Meng, Q. Numerical Investigations on the Influence of Superimposed Double-Sided Pressure on the Formability of Biaxially Stretched AA6111-T4 Sheet Metal. *J. Mater. Eng. Perform.* **2011**, *21*, 429–436. [CrossRef]